ChemComm

COMMUNICATION

View Article Online
View Journal | View Issue

Cite this: *Chem. Commun.*, 2015, **51**, 15925

Received 13th August 2015,
Accepted 3rd September 2015

DOI: 10.1039/c5cc06805c

www.rsc.org/chemcomm

Dynameric asymmetric membranes for directional water transport†

Yan Zhang and Mihail Barboiu*

Hydrophilic/hydrophobic dynamers prepared *via* template partial phase segregation have been used in the formation of asymmetric membranes for directional water transport.

Dynamic polymers – dynamers,[1–4] have emerged as a new class of reversible materials giving access to adaptive behaviours in response to external[5–11] or internal stimuli, leading to specific structures and variable morphologies.[12,13] Recently we became interested in biomimetic water transport which may imply important insights into solving important biological scenarios and also providing an improvement over current technologies in water desalination.[14–16] Wetting behaviours in natural systems (*i.e.* lotus leaves, butterfly wings, *etc.*) are other inspiring examples for the construction of systems for water transport.[17–20] We know that the directional water transport can be achieved by using hydrophobic/hydrophilic HP/HY porous macroscopic layers.[20] Within this context, we considered that dynameric membranes prepared under molecular control[6] may constitute interesting alternatives in the ability to control directional water transport and to go further toward highly selective separation of low mass solutes (ions, peptides, *etc.*) controlled *via* molecular diffusion.

Herein, we report asymmetric HP/HY dynameric membranes for directional water transport. We presumed that the combination of HP and HY segments connected *via* reversible covalent bonds may induce phase segregation at the molecular level in the presence of a templating support, under the pressure of constitutional internal affinity of components. In order to generate such dynamers, trialdehyde core-centres, HY PEG-diamine and HP alkane-diamine segments have been connected *via* reversible amino-carbonyl/imine chemistry. This results in the formation of dynameric frameworks, enabling the dynamic exchange between components in solution and gels toward membrane formation by casting on templating support. Using such constitutional reorganization during the phase change processes,[21] partial phase segregation can be achieved at the molecular level (Fig. 1). Our initial attempt started with 1,3,5-benzenetrialdehyde **1**, and 2,2′-(ethylenedioxy) bis(ethylamine) **2**, (0.75 eq.) and 1,8-diaminooctane **3** (0.75 eq.) building blocks (reflux 2 h, in $CHCl_3$ – Scheme 1a). ^{1}H-NMR spectral data agree with the total consumption of aldehydes and the formation of symmetrical cross-linked **1·2·3** frameworks (Fig. S3 and S4, ESI†). HP Teflon plates have been used as templating surfaces. In order to examine the molecular segregation effect, we used the contact angle analysis (CA) as a direct indication of wettability behaviours, as well as energy-dispersive X-ray spectroscopy (EDX) to know the elemental distribution on both membrane surfaces. The CA shows that the wettabilities of the membrane air-contact upside surface and down-side support-contact surface are almost similar: 80.9° and 88.0° (Teflon) or 76.7° and 80.2° (glass), respectively, in agreement with EDX atomic distribution (ESI†) proving that for these precursors the constitutional interactions of the short chains are not strong enough in order to promote segregation.

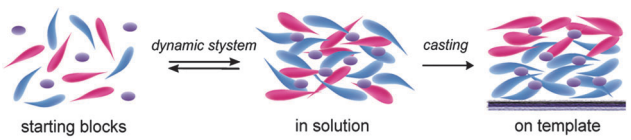

Fig. 1 Constitutional segregation of the hydrophilic (blue)/hydrophobic (red) elements connected *via* core-centres (violet) for asymmetric membrane generation.

Considering the moderate segregation observed for **1·2·3**, longer molecular components 4,7,10-trioxa-1,13-tridecane-diamine **4** and 1,12-diamino-dodecane **5** were used thereafter using similar experimental conditions (Scheme 1b). In this case, solvents with different polarities were screened: $CHCl_3$, CH_3CN, THF and acetone. ^{1}H-NMR spectral data agree with the partial consumption of aldehydes and the formation of unsymmetrical cross-linked **1·4·5** frameworks (Fig. S5–S7, ESI†). From the results of CA, all membranes **1·4·5** showed considerable improvement in phase

Institut Européen des Membranes, ENSCM-UM-CNRS, Adaptive Supramolecular Nanosystems Group, Place Eugène Bataillon, CC 047, F-34095 Montpellier, France. E-mail: mihail-dumitru.barboiu@univ-montp2.fr

† Electronic supplementary information (ESI) available: NMR, SEM, EDX contact angle and water transport experiments. See DOI: 10.1039/c5cc06805c

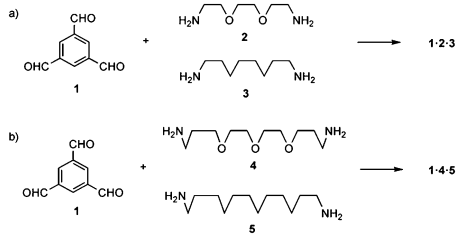

Scheme 1 Schematic representation of the synthesis of dynameric frameworks combining (a) 1,3,5-benzenetrialdehyde **1**, and 2,2′-(ethylenedioxy)-bis(ethylamine) **2**, and 1,8-diaminooctane **3** and (b) 1,3,5-benzenetrialdehyde **1**, 4,7,10-trioxa-1,13-tridecanediamine **4**, and 1,12-diaminododecane **5**.

segregation compared to **1·2·3**. For example with $CHCl_3$, the contact angle of the upside surface was 36.72°, and the value from the down-side surface was 71.90°. Besides this, for the membrane generated from CH_3CN, water disappeared quickly on the upside surface showing high wettability, while the contact angle of the down-side of the membrane was 86.21°. Furthermore, the EDX data clearly demonstrated the uneven elemental distribution between the two sides (Table 1). However we note that the CA values are reminiscent with a partial segregation behavior as time as the HY CA values are not very low and HP CA angles are not very high. Along the phase segregation process, the hydrophilic amino and PEG groups tend to gather together on the HY region of the membrane, leaving most of the hydrophobic alkane groups on the HP region of the membrane. HY/HP and HY/HP dominant/residual behaviors are generated at the molecular level toward the hybrid distinct surfaces of the material. We noted that the difference between membrane upside and downside surfaces is a general trend and strongly dependent on the solvent used (Table 1).

The morphology obtained from scanning electron microscopy (SEM) further confirmed that membranes (100–200 μm) present dense surfaces, without pinholes or pores. Among the solvents tested, the membrane generated from CH_3CN showed an important difference between the two sides of different morphological behaviors. Even through the naked eye, the upside of the membrane presented as a rough surface, at the same time the down-side of the membrane appeared very smooth (Fig. 2). This interesting behavior is not only attributed to the polarity of CH_3CN, favoring molecular

Table 1 EDX results for membranes generated from different solvents

		CA[a] (°)	C[b]	N	O
CH_3CN	Upside	—[c]	78.14	10.62	11.24
	Down-side	86.2	83.45	9.68	6.87
$CHCl_3$	Upside	36.7	87.87	2.40	9.73
	Down-side	71.9	89.11	1.55	9.34
THF	Upside	49.6	78.82	10.97	10.21
	Down-side	65.3	80.82	10.57	8.61
Acetone	Upside	40.6	72.82	15.22	11.96
	Down-side	80.4	75.71	13.70	10.58

[a] Contact angles were measured using water droplets on the surface of the membrane. [b] The recorded data are in atomic percentages. [c] Water droplets disappeared quickly on the membrane surface.

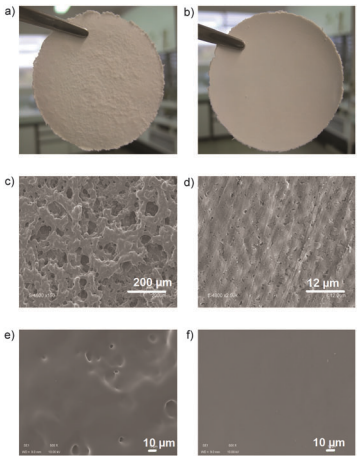

Fig. 2 The images of upside (a) and down-side (b) of membrane **1·4·5**; the SEM images of the upside (c) and down-side (d) of membrane **1·4·5**; the SEM images of the upside (e) and down-side (f) of membrane **1·4** as comparison.

segregation, but also to the kinetics of the evaporation process. The difference in the morphological surface behaviors is still present in the cases of the other solvents, resulting in the formation of less tortuous non-porous upside surfaces (Fig. S9, ESI†). Importantly the same experiment conducted for a mixture of **1·4** (molar ratio of 1 : 1.5) casted from CH_3CN results in the formation of tight non-porous morphologies on both the sides (Fig. 2e and f). CA showed that water quickly disappeared from both sides of membrane **1·4** and EDX gave almost the same elemental distribution for the two sides.

The membranes saturated in water for 2 h have been evaluated for their transport properties by using a Sterlitech HP4750 stirred cell, connected with a balance to measure the water mass transported through the membrane. The total water mass *versus* time profiles have been used to determine the flux of water filtered through the membranes, oriented with the upside or downside surface to the water stream (Fig. 3). Interestingly, at a low pressure of 0.007 bar, water is transported only when the upside surface of membrane **1·4·5** casted from CH_3CN is exposed to water, with a mass flux of 0.630 g min^{-1} (Fig. 3c), while is completely blocked from the down-side surface of the membrane (Fig. 3c). The water permeability is favored for the upside surface of the membrane (P = 7400 L m^{-2} h^{-1} bar^{-1}). When higher pressures are applied, water fluxes are increasing and water can also slowly penetrate from the down-side (P = 3900 L m^{-2} h^{-1} bar^{-1}). For the reference membrane **1·4** casted from CH_3CN we recorded similar permeabilities (P = 18 L m^{-2} h^{-1} bar^{-1} and P = 14 L m^{-2} h^{-1} bar^{-1} respectively) for the two sides (Fig. 3d). The membranes casted from other less polar solvents than CH_3CN give less different permeabilities between the two sides, in accordance with CA and EDX data, showing less phase segregation at the molecular level (Table 2 and Fig. S10, ESI†). We point out the high values of water permeability obtained with these membranes that would make them potential candidates for the separation of other solutes like ions, peptides, proteins or other metabolites.[22] The mechanism of water permeability is different from the related previous studies on porous systems,[20] and is mostly related to

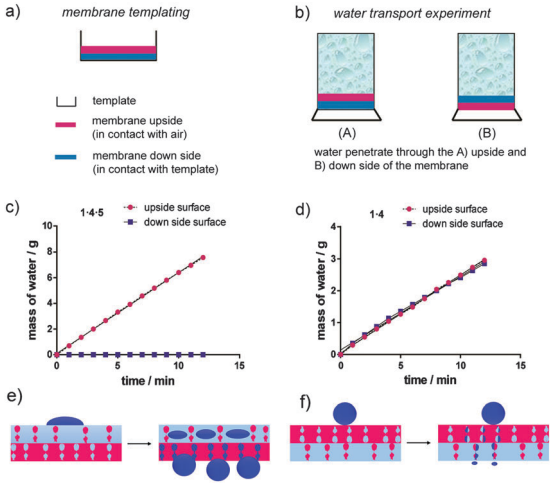

Fig. 3 Water transport experiment for the two sides of the membrane: schematic presentation of (a) the two sides of the membrane and (b) water transport directions; water flux of the two sides of membranes (c) **1·4·5** and (d) **1·4**; mechanism of preferential water permeation of (e) wettable HY surface and of (f) unwettable HP surface.

Table 2 Water permeability of **1·4·5** obtained from different solvents and **1·4** from CH_3CN[a]

		Upside surface[b] (L m^{-2} h^{-1} bar^{-1})	Down-side surface[c] (L m^{-2} h^{-1} bar^{-1})
1·4·5	CH_3CN	7400	3900
	Acetone	25	31
	$CHCl_3$	160	71
1·4	CH_3CN	18	14

[a] For the calculation method see ESI. [b] Water penetrates through the upside surface. [c] Water penetrates through the down-side surface.

the wettability and to the dominant/residual HY/HP or HP/HY hybrid structures of the dense surfaces. If water is dropped on the dense non-porous HY surface, it spreads and absorbs into the film. This effect is amplified by the roughness of the HY surface of membrane **1·4·5**, casted from CH_3CN showing one/two orders of magnitude higher permeability than other membranes with smooth surfaces. Although the HP region would tend to block the water penetration, the increased accumulation of water in the HY region will then reach the residual HY channels of the HP part overcoming the hydrophobic forces and penetrating the whole membrane (Fig. 3e). Differently, the accumulation of water in the HY residual part of the HP region is probably not sufficient for reaching a critical water volume to overcome the hydrophobic forces and to penetrate the HY part of the membrane (Fig. 3f). However this blockage is overcomed by increasing the operating pressure which increases the water permeability from the HP side.

All these results demonstrate that the synergetic incorporation of hydrophobic/hydrophobic components is crucial for the template induced phase segregation within the structure of the dynameric frameworks for asymmetric membrane preparation. This process is strongly dependent on the solvent used and is supported by CA, EDX, SEM, and experimental results. Its application in directional water transport was further confirmed. At low pressure, water can only penetrate through the HY side of the membrane and is blocked from the HP side. Straightforward synthetic access to asymmetric membranes gives rise to novel strategies to constitutionally build up under molecular control very productive transport membranes for high value added applications such as water purification or protein purification.

This work was supported by funds from ITN DYNANO, PITN-GA-2011-289033 (www.dynano.eu) and Agence National de Recherche, ANR-DYNAFUN.

Notes and references

1 J. Lehn, *Aust. J. Chem.*, 2010, **63**, 611–623.
2 J.-M. Lehn, *Angew. Chem., Int. Ed.*, 2013, **52**, 2836–2850.
3 R. Catana, M. Barboiu, I. Moleavin, L. Clima, A. Rotaru, E.-L. Ursu and M. Pinteala, *Chem. Commun.*, 2015, **51**, 2021–2024.
4 *Constitutional Dynamic Chemistry*, ed. M. Barboiu, Springer Verlag, Berlin, 2012.
5 T. Aida, E. W. Meijer and S. I. Stupp, *Science*, 2012, **335**, 813–817.
6 G. Nasr, M. Barboiu, T. Ono, S. Fujii and J.-M. Lehn, *J. Membr. Sci.*, 2008, **321**, 8–14.
7 N. Roy, E. Buhler and J.-M. Lehn, *Chem. – Eur. J.*, 2013, **19**, 8814–8821.
8 J. Yang, Z. Li, Y. Zhou and G. Yu, *Polym. Chem.*, 2014, **5**, 6645–6650.
9 E. Kolomiets and J.-M. Lehn, *Chem. Commun.*, 2005, 1519–1521.
10 S. Dong, Y. Luo, X. Yan, B. Zheng, X. Ding, Y. Yu, Z. Ma, Q. Zhao and F. Huang, *Angew. Chem., Int. Ed.*, 2011, **50**, 1905–1909.
11 M. J. Barthel, T. Rudolph, A. Teichler, R. M. Paulus, J. Vitz, S. Hoeppener, M. D. Hager, F. H. Schacher and U. S. Schubert, *Adv. Funct. Mater.*, 2013, **23**, 4921–4931.
12 C.-F. Chow, S. Fujii and J.-M. Lehn, *Chem. Commun.*, 2007, 4363–4365.
13 D. Janeliunas, P. van Rijn, J. Boekhoven, C. B. Minkenberg, J. H. van Esch and R. Eelkema, *Angew. Chem., Int. Ed.*, 2013, **52**, 1998–2001.
14 (*a*) Y. Le Duc, M. Michau, A. Gilles, V. Gence, Y.-M. Legrand, A. van der Lee, S. Tingry and M. Barboiu, *Angew. Chem., Int. Ed.*, 2011, **50**, 11366–11372; (*b*) M. Barboiu, *Angew. Chem., Int. Ed.*, 2012, **51**, 11674–11676.
15 M. Barboiu and A. Gilles, *Acc. Chem. Res.*, 2013, **46**, 2814–2823.
16 M. Barboiu, *Eur. J. Inorg. Chem.*, 2015, 1112–1125.
17 X. J. Feng and L. Jiang, *Adv. Mater.*, 2006, **18**, 3063–3078.
18 X. Yao, Y. Song and L. Jiang, *Adv. Mater.*, 2011, **23**, 719–734.
19 L. Jiang, Y. Zhao and J. Zhai, *Angew. Chem., Int. Ed.*, 2004, **116**, 4438–4441.
20 J. Wu, N. Wang, L. Wang, H. Dong, Y. Zhao and L. Jiang, *Soft Matter*, 2012, **8**, 5996–5999.
21 (*a*) L. Marin, B. Simionescu and M. Barboiu, *Chem. Commun.*, 2012, **48**, 8778–8780; (*b*) S. Mihai, A. Cazacu, C. Arnal-Herault, G. Nasr, A. Meffre, A. van der Lee and M. Barboiu, *New J. Chem.*, 2009, **33**, 2335–2343; (*c*) L. Hu, Y. Zhang and O. Ramström, *Sci. Rep.*, 2015, **5**, 11065, DOI: 10.1038/srep11065.
22 A. Mehta and A. L. Zydney, *J. Membr. Sci.*, 2005, **249**, 245–249.